Chemical Physics Letters 503 (2011) 256–261

Contents lists available at ScienceDirect

Chemical Physics Letters

journal homepage: www.elsevier.com/locate/cplett

Fluorescence correlation spectroscopy near individual gold nanoparticle

Qingyan Wang [a], Guowei Lu [a,*], Lei Hou [a], Tianyue Zhang [a], Chunxiong Luo [a], Hong Yang [a], Grégory Barbillon [b], Franck H. Lei [c], Christophe A. Marquette [d], Pascal Perriat [e], Olivier Tillement [f], Stéphane Roux [f], Qi Ouyang [a], Qihuang Gong [a,*]

[a] Department of Physics, State Key Laboratory for Mesoscopic Physics, Peking University, 100871 Beijing, China
[b] Laboratoire Charles Fabry de l'Institut d'Optique, LCFIO CNRS UMR 8501, Institut d'Optique Graduate School, RD 128 – Campus Polytechnique, 2 avenue Augustin Fresnel, 91127 Palaiseau Cedex, France
[c] Unité MéDIAN, UFR Pharmacie, Université de Reims Champagne-Ardenne, UMR CNRS 6237, 51 rue Cognacq-Jay, 51096 Reims Cedex, France
[d] Institut de Chimie et Biochimie Moléculaires et Supramoleculaires, Université Lyon 1 – CNRS 5246 ICBMS, Bâtiment CPE 43, bd du 11 novembre 1918, 69622 Villeurbanne Cedex, France
[e] MATEIS (GEMPPM) – UMR CNRS 5510, INSA de Lyon, Batiment Blaise Pascal, 7 avenue Jean Capelle, 69621 Villeurbanne Cedex, France
[f] Laboratoire de Physico-Chimie des Matériaux Luminescents, Université Claude Bernard Lyon I, 69622 Villeurbanne Cedex, France

ARTICLE INFO

Article history:
Received 11 September 2010
In final form 2 January 2011
Available online 4 January 2011

ABSTRACT

Dynamic behavior of fluorescent molecules near an individual gold nanoparticle is investigated experimentally by fluorescence correlation spectroscopy method. The gold particle that acts as an optical nano-antenna presents significant near-field volume reduction. The single molecule diffusion behavior is clearly observed within a reduced near-field volume due to a highly localized field enhancement. The near-field volume and fluorescence enhancement are polarization and concentration dependent and strongly depend on the properties of the gold nanoparticle. A simple approximated model is developed to fit the FCS autocorrelation curves. In principle, the single molecule analysis within the near-field volume of nanostructures could be applied to the analysis of biological membranes and intracellular processes.

1. Introduction

Spectroscopic technique with single molecule sensitivity provides unique advantages to understand biochemical or microbiological process. Various optical techniques have been recently developed with sufficient sensitivity to detect single molecules. Fluorescence correlation spectroscopy (FCS) introduced in the early 70's by Magde, Elson and Webb has become a very attractive and widespread tool that reaches single molecule sensitivity in studies of biological processes on a subcellular level [1–4]. Recently, many efforts were devoted to reduce the effective detection volume and increase the signal to noise ratio for single molecule analysis at high concentration in vitro or in vivo. For example, nanoscale detection volume generated by stimulated emission depletion, mechanically confined sampling volume by sub-microfluidic channels, and total internal reflection were introduced into the FCS technique [5–7]. Moreover, the nanophotonics offers the FCS technique new opportunities to reduce the detection volume or increase the fluorescence count rate per molecule. For instance, isolated nanometric circular holes milled in metallic films were applied for single molecule analysis in a highly concentrated solution with standard FCS techniques [8–10]. Optical probe with nano-apertures or bare fiber tip under the control of scanning near-field microscope was integrated successfully with FCS technique and applied in membrane behaviors studies [11–14]. The interference fringes of an excitation beam near the metal surface [15] and the nano-fakir metal surfaces were also applied in FCS researches [16]. Interestingly, in the vicinity of the metallic nanostructure, the excitation of the local mode of the surface plasmon can lead to an enhancement of the electric field and modify the quantum yield of single molecules. Extensive experiments have shown that the fluorescence or Raman scattering of molecules is greatly enhanced by rough metallic films or particles [17–21]. However, in most of the previous studies, the fluorophore is immobilized in the vicinity of nanostructures, for example, connected to the silver nanoparticles by long-chain molecules (e.g. DNA in Ref. [18]), or fixed in a matrix (e.g. PMMA in Ref. [21]) coating onto the nanostructure. Recently, Estrada et al. reported the investigation of the free diffusing fluorophores within the intrinsic near-field volume around the gold nanoparticles [20]. They showed that the presence of individual gold nanoparticles permitted to reduce the detection volume by 4 orders of magnitudes due to the localized surface plasmon resonance of the gold nanoparticles, which would result in the confinement of the electromagnetic waves below the diffraction limit in the vicinity of the nanoparticle. However, the

* Corresponding authors.
E-mail addresses: guowei.lu@pku.edu.cn (G. Lu), qhgong@pku.edu.cn (Q. Gong).

0009-2614/$ - see front matter © 2011 Elsevier B.V. All rights reserved.
doi:10.1016/j.cplett.2011.01.005

heavy surface adsorption of the dye molecules hindered the researchers to extract accurate dynamic information because of a high background noise and the molecule surface adsorption effect.

In this work, the single molecule dynamic behaviors near an individual AuNP are investigated without the surface adsorption effect by fluorescence correlation spectroscopy experimentally. Our experimental results truly reveal that the near-field volume due to the local surface plasmon of the AuNP is significantly reduced compared to that of the conventional confocal instrumentation, and the molecule diffusion process can be observed undoubtedly within such near-field volume. A simple theoretical analysis is developed to characterize the autocorrelation curves. Moreover, the polarization dependence of the near-field FCS is investigated in detail at various fluorescence dye concentrations.

2. Instruments and methods

Figure 1a outlines our confocal FCS setup with a piezo *xy*-translation stage based on NTEGRA Spectra system (NT-MDT, Russia). Here, the beam of a HeNe laser (CW laser, λ: 633 nm) was enlarged by means of a telescope and focused with an oil immersion objective lens (NA = 1.4, 100×, Olympus, Japan). Fluorescence light was collected by the same objective, passed through a dichroic mirror and a bandpass emission filter (LPD01-633RU, FF01-661/20–25, Semrock) to block the reflected laser light, and was focused onto the end of a fiber with a core diameter of 50 μm. The core of the fiber acts as a pinhole assuring the confinement of the observation volume. A 50/50 fiber splitter was used to send the signal to two avalanche photodiodes (SPCM-AQRH-16-FC, PerkinElmer) for cross-correlation to suppress afterpulsing (correlator.com, US). At the same time, a CW laser at the wavelength of 532 nm (LCM-S-111, Laser-export Co. Ltd.) was focused by the same objective lens collinearly for confocal scanning images. The optical signal was collected in reflection, passed through a beam splitter, and focused by a lens onto a diameter-variable confocal pinhole. A photomultiplier (Hamamatsu, H5784-04) built in the NTEGRA Spectra system detected the signal of the interferences between the lights scattered by the AuNP and the substrate surface [22].

The conventional FCS scheme typically uses the diffraction-limited optics to probe single molecule dynamics in fluid observation volumes. The unprecedented ability of metallic nano-structures to concentrate light into deep-subwavelength volumes provides a way for FCS technique to significantly reduce the observed volume. Here, we used a spherical AuNP attached onto a coverslip to produce highly confined optical field in the vicinity of the AuNP. In the calculations, the AuNP was considered as a sphere although the real AuNP used in the experiment was not perfectly spherical. Three dimensional FDTD simulations were performed to reveal the electric field intensity contours near a nanoparticle with a diameter of 60 nm. The AuNP was illuminated by the tightly focused Gaussian laser beam at the wavelength of 633 nm with the linear polarization along the *x* axial direction. Figure 1b shows that the electric field intensity near the surface of the AuNP is higher than that of the illuminating Gaussian profile, and that the extension of the enhanced electric field is confined tightly near the AuNP surface. Since the emission of the dye molecule near the AuNP is distance dependent, the enhancement of fluorescent signal only happens at the proper distance between the dye molecule and the AuNP. That would result in an additional fluorescence signal fluctuation near the AuNP expect for the fluorescence fluctuation in the far-field volume directly. It would allow a near-field FCS measurement with an observation volume below the optical diffraction limit.

FCS autocorrelation function is defined as $G_{(\tau)} = \langle F_t \cdot F_{t+\tau} \rangle / \langle F \rangle^2$ based on the measurement of the equilibrium fluctuations of the detected fluorescence intensity F_t.

For the fluorophores freely diffusing in solution, $F_t = \int Q_r \cdot I_r \cdot C_{r,t} dV$ is determined by the fluorophore concentration $C_{r,t}$, the specific brightness Q_r (the product of the absorption cross section by the fluorescence quantum yield, and the detection efficiency), and by the profile of the excitation light I_r (in fact, I_r is determined by both the illumination and the detection optical paths). In the conventional FCS scheme, the specific brightness Q_r is a constant and the analytical approximation of I_r is simply given by the 3D Gaussian profile $I_r = I_0 \exp\left(-2\frac{x^2+y^2}{\omega_{xy}^2} - 2\frac{z^2}{\omega_z^2}\right)$. On the contrary, in the presence of a nanoparticle, Q_r and I_r are position and polarization dependent on the properties of the local surface plasmon resonance of the nanostructure [17–20,23,24]. As shown in Figure 1b, the field distribution of the excitation light is modified by the AuNP. Because the modifications of Q_r and I_r only happen in the very vicinity of the particle, the excitation profile can be approximately separated into two Gaussian profile parts: $I_{1,r}$ (ω_{1_xy}, ω_{1_z}) for the far-field focused spot related to the objective lens directly and $I_{2,r}$ (ω_{2_xy},ω_{2_z}) representing the effective near-field

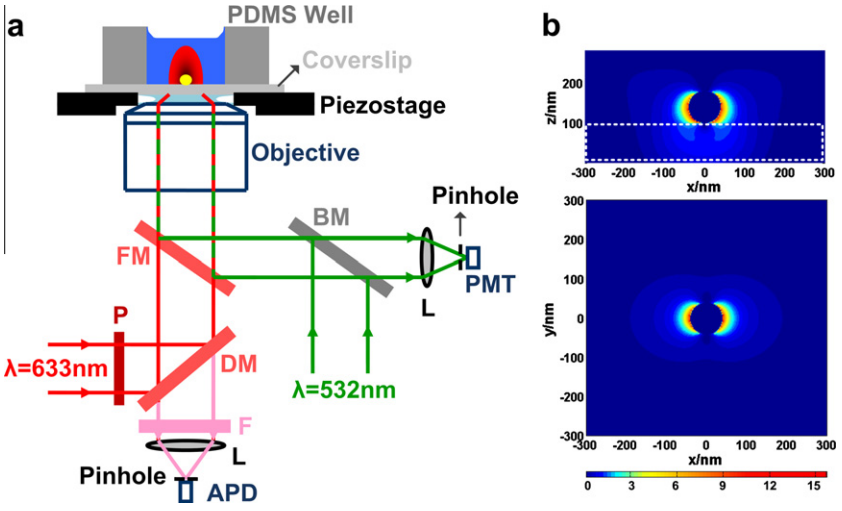

Figure 1. (a) Schematic representation of the setup for the near-field FCS with single gold nanoparticle. P, $\lambda/4$ plate; L, lens; F, fluorescence filters, FM, flip mirror; BM, beamsplitter mirror; DM, dichroic mirror. (b) Electric field intensity distributions near a gold nanoparticle simulated by 3D FDTD method. The space is divided by $\Delta x = \Delta y = \Delta z = 2$ nm. The nanoparticle on the glass substrate with $\varepsilon = 2.3$ is illuminated by a focused Gaussian beam with linear polarization along the *x* axis.

distribution around the AuNP. The parameter Q_r is assumed to remain a constant Q_c in the far field, but it is position and polarization dependent within the near field of the AuNP. In the first approximation, the fluorescence enhancement factor ρ_r induced by the AuNP in the near field is assumed to be a constant when deriving the autocorrelation function. Then the detected fluorescence intensity in the presence of the AuNP can be written as $F_t \approx \int Q_c \cdot (I_{1,r} + \rho_r \cdot I_{2,r}) \cdot C_{r,t} dV$. Thus the autocorrelation function is given by the following formula [25,26]:

$$G(\tau) = 1 + \left[1 + P_T \exp\left(-\frac{\tau}{\tau_T}\right)\right] \frac{(1 - \langle B\rangle/\langle F\rangle)^2}{(N_1 + \rho_r N_2)^2} \times \left[\frac{N_1}{(1+\tau/\tau_1)\sqrt{1+\tau/s_1^2\tau_1}} + \frac{N_2\rho_r^2}{(1+\tau/\tau_2)\sqrt{1+\tau/s_2^2\tau_2}}\right] \quad (1)$$

where $s_1 = \omega_{1-z}/\omega_{1-xy}$, $s_2 = \omega_{2-z}/\omega_{2-xy}$, $\tau_1 = \omega_{1-xy}^2/4D$, $\tau_2 = \omega_{2-xy}^2/4D$, D is the diffusion coefficient, N_1 is the number of the fluorescent molecules in the far-field volume due to the objective lens illumination $V_1 = \frac{1}{2}\pi^{3/2}\omega_{1-xy}^2\omega_{1-z}$ taking account of the mechanical confinement by the coverslip, N_2 is the number of the fluorescent molecules in the near-field volume around the AuNP, $V_2 = \pi^{3/2}\omega_{2-xy}^2\omega_{2-z}$, $\langle F\rangle$ is the total signal, $\langle B\rangle$ is the background noise which is measured for the pure water without any fluorophore dye, p_T is the amplitude of the dark state population including the trans–cis isomerization and singlet–triplet transitions processes, and τ_T is the dark state blinking time as an approximation for these effects. In the absence of particles ($\rho_r = 0$), the autocorrelation $G_{(\tau)}$ returns to the conventional free Brownian three-dimensional diffusion in a single Gaussian excitation profile.

3. Experimental results and discussions

3.1. Preparation of AuNPs-immobilized substrate

In this work, gold nanoparticles with diameter of 60 ± 10 nm were synthesized by the citrate reduction method [27]. The size and the shape of the synthesized AuNPs were characterized by a transmission electron microscopy (TEM, Hitachi H-9000). A typical TEM image of the synthesized gold colloid nanoparticles is shown in Figure 2a. The extinction spectra of the colloids were measured by Agilent 8453 UV–Visible spectrophotometer, and one example is shown in Figure 2b. Let us point out that the ensemble extinction spectrum of the AuNPs used in this experiment presents an overlap with the excitation laser and the emission band of the Cy5 molecule. Tuning the resonance peak of the AuNP to match the excitation or emission band of the system should result in higher enhancement efficiency, which is beyond the scope of this paper. Then, the AuNPs were immobilized onto the glass coverslips through 3-aminopropyl-trimethoxysliane (APTMS), the particle and the glass surface were linked together through the surfactant APTMS [28]. Briefly, a coverslip was cleaned carefully before an oxygen plasma treatment and immersed in 1% (v/v) APTMS solution for 30 min. After silanization of its surface, a droplet containing the AuNPs was deposited onto the APTMS-functionalized coverslip, and stayed for 3 min to form a sparse coverage of the AuNPs. Then the coverslip was washed thoroughly with ethanol and water to remove the unbinding AuNPs. The prepared substrate was treated by oxygen plasma technique again to prevent unspecific binding and next a PDMS liquid well was attached onto the coverslip to hold the fluorophore solution. The AuNPs-immobilized coverslips were characterized by the confocal scan method, which is described in Ref. [22]. A typical image is presented in Figure 2c with an area of 30 × 30 μm, and the results reveal that the AuNPs

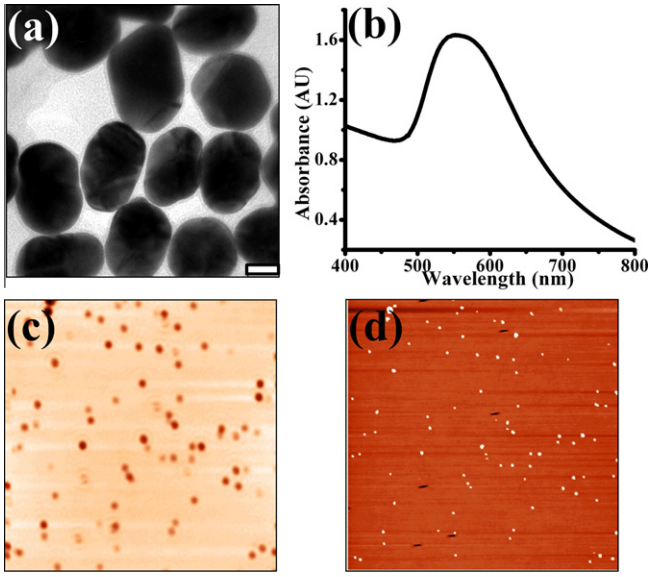

Figure 2. (a) TEM image of the gold nanoparticles used in this experiment. The scale bar is 30 nm. (b) Extinction spectrum of the synthesized gold colloid solution. (c) Laser confocal scan of a sample containing gold nanoparticles immobilized on the coverslip with an area of 30 × 30 μm. (d) AFM image of the same area as the confocal image.

are immobilized on the glass surface successfully. In order to confirm it further, atomic force microscopy (AFM) scanning was performed at the same area with tapping mode based on NTEGRA Spectra system (see Figure 2d). The AFM results show that the nanoparticles have the same height distribution (data not shown here) as compared to the size distribution measured by TEM. The positions of the nanoparticles are consistent with the results obtained by the confocal scan method. Moreover, AFM image with high resolution was performed to reveal that most of the immobilized AuNPs onto the surface were isolated, and aggregation happened sparsely. Also, the scanning optical images in the aqueous solution obtained with overnight interval verified that the AuNPs are well immobilized on the surface. The background noise in presence of AuNPs alone was measured using pure water before the aqueous dye solution was added. The background in the presence of the AuNP is higher than 1.8 kHz for the most of particles at the excitation power of 10 μW, which are various for the different particle. In the absence of the AuNP, the background near the glass surface is about 1.3 kHz at the excitation power of 10 μW. All these background signals were not found to present any autocorrelation.

3.2. Single molecule FCS measurements near single AuNP

With the help of the confocal scan images based on NTEGRA Spectra system, FCS measurements can be performed at a high spatial accuracy with or without AuNP. At first, we ensured that the spot was focused at the interface in the absence of particles. Secondly, the sample was translated in lateral directions using the piezo-stage to move the AuNP into the focus spot. We can also map the FCS measurement around a single AuNP to check this [13]. For 45 nM Cy5 solution, Figure 3 shows the typical results obtained. First of all, the fluorescence intensity shown in Figure 3a increases obviously in the presence of AuNP as compared to that without it, and the fluorescence intensity-time trace has clear fluorescence bursts probably due to single or several dye molecules diffusing close to the nanoparticle. Second, with an excitation laser power varying from 1 to 30 μW, the evolution of the fluorescence

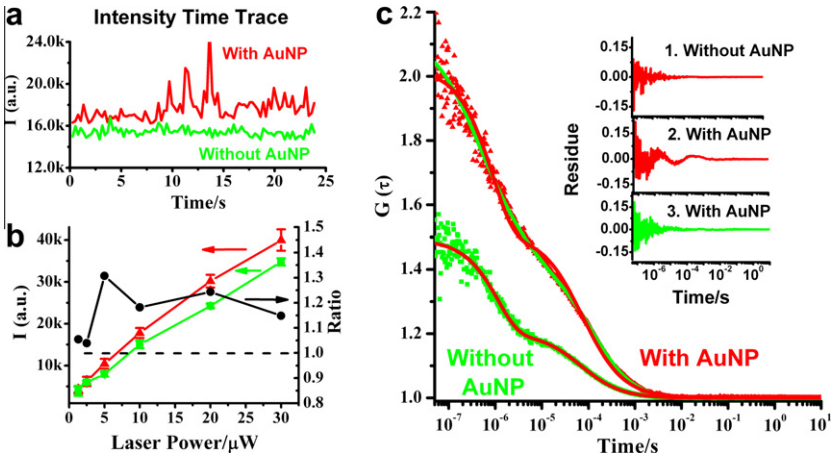

Figure 3. (a) Typical fluorescence intensity-time traces for the 45 nM Cy5 solution with an AuNP (red) and without anyone (green). The excitation power is 10 μW. (b) Fluorescence intensities versus the excitation laser power. The red ones are for the experimental data with an AuNP, the green ones are for that without any AuNP, and the black ones indicate the ratio of the red ones to the corresponding green ones. (c) Typical original FCS autocorrelation data with an AuNP (red triangles) and without anyone (green squares). The red lines are the fitting curves with the standard 3D Gaussian model, and the green line is the fitting curve with Eq. (1), viz. taking into account the presence of an AuNP. Insets 1 and 2 show the residues of the fittings with 3D Gaussian model, while inset 3 is for the fitting with Eq. (1). (For interpretation of the references to colour in this figure legend, the reader is referred to the web version of this article.)

intensity is shown in Figure 3b. Under such a low excitation power, since the value of $G_{(0)}$ and the diffusion time remain constant when the excitation power changes, the conditions leading to the photobleaching are avoided here. The maximum enhancement ratio γ is about 1.3 at 5 μW (the black line), and the actual average fluorescence enhancement factor could be estimated as $\frac{V_1}{V_2}(\gamma - 1)$. Although the fluorescence enhancement phenomena were extensively investigated with experiments and theories, it is still difficult to estimate the near-field volume by the calibration of spontaneous emission rate and fluorescence enhancement efficiency. In the present work, it is thought that the diffusion time is a reliable parameter that can be extracted from the ACF curves rather than the enhancement factor. In the fitting procedure, the diffusion time τ_1 was restricted within 30–300 μs because it represents the far-field volume by the objective lens directly. And the diffusion time τ_2 was restricted within 1–30 μs, because it's well known that the near-field around the AuNPs which decays exponentially within 10–30 nm along the direction perpendicular to the surface. Then, the spatial scale of the detection volume can be estimated according to the diffusion equation: $\tau = \omega^2/4D$, so that one can compare the far-field volume with the near-field volume.Here, single molecule FCS measurement can provide the experimental information to a considerable extent. Figure 3c shows that the autocorrelation curve near an AuNP is significantly changed compared with that in the absence of the particle. The value $G_{(0)}$ increases clearly, which results from the highly confined optical fields near the surface of the AuNPs. The red solid lines are the fitting curves with Eq. (1) ($\rho_r = 0$), i.e. the conventional three dimensional Brownian diffusion in a Gaussian profile. It fits the FCS data in the absence of AuNPs well ($\tau_1 = 70 \pm 10$ μs and $\tau_T = 1.0 \pm 0.2$ μs are obtained), but cannot fit correctly the data in the presence of AuNP (see Figure 3c insets). Instead, the red triangles are well fitted by the full Eq. (1) that takes into account the presence of the particles. The parameters: $s_1 \approx 8$, $s_2 \approx 0.2$, $\tau_1 = 100 \pm 15$ μs, $\tau_2 = 6.5 \pm 2.0$ μs, were obtained, and $\tau_T = 1.0$ μs is fixed during the fitting. It should be noted that the triplet dark state blinking and trans–cis isomerization effect of Cy5 molecule could be modified by the presence of the AuNP even the illumination laser source was kept at the same level. Since both the FCS curves with or without the AuNP were obtained at low excitation power (about 10 μW), these dark state blinking effects are simplified here as an approximation by fixing the τ_T around 1.0 μs [29]. The τ_1 for the far-field volume in the presence of an AuNP is longer than that in the absence of AuNP, which could be attributed to the particle acting as an obstacle for the diffusing dye molecules, thus leading to an increase of the residence time of the molecules in the detection volume [26]. As is well known, the longitudinal scale of Gaussian shape in the far field related to the objective lens is usually longer than that of the lateral ones, so that the value of $s_1 \approx 8$ is reasonable. On the contrary, the ratio $s_2 = \omega_{2-z}/\omega_{2-xy}$ for the near-field volume around the AuNP is about 0.2, much less than 1. It implies that the longitudinal scale perpendicular to the surface of the AuNP is shorter than that of the lateral ones along the surface of the AuNP. In general, the confined near field decays exponentially in the perpendicular direction, but spreads near the surface of the sphere, which is in agreement with the FDTD simulations in Figure 1b. Moreover, the actual near-field volume can be roughly estimated by the diffusion time $\tau_1 = \omega_{1-xy}^2/4D$. Assuming that the diffraction limit ω_{1-xy} is about 280 nm for the far field, then the ω_{2-xy} is about 85 nm for the shorter diffusion time: $\tau_2 = 6.5 \pm 1.0$ μs, and ω_{2-z} is about 17 nm according to the ratio $s_2 \approx 0.2$. Strictly, the fitting model used here is not exact completely, but the approximation seems to work well. The near-field volume of the AuNP is about 3 orders of magnitude smaller than that of the far-field volume. Thus the single molecule FCS results are truly able to represent the electromagnetic field distribution in the vicinity of an individual AuNP. As discussed in above paragraph, it is difficult to obtain the real enhancement factor for each AuNP. And the N_2 and ρ_r are strong covariance making it impossible to fit the two parameters simultaneously. The value of N_2, the molecule number in the near-field volume, can be derived from the ratio of the near-field volume to the far-field volume. Then, the enhancement factor can be obtained through the value of N_2 derived from the near-field volume (given that the dye molecule concentration is homogenous for both far- and near-field volume). In the fitting procedure, the value of N_2 is dependent on the value of the fluorescence enhancement factor ρ_r (e.g. if $\rho_r = 50$ is fixed, $N_1 \approx 2.2 \pm 0.1$ and $N_2 \approx 0.0014 \pm 0.0002$ are obtained). That means more enhancement efficiency representing a smaller near-field volume, and the factor ρ_r can be estimated by setting the ratio of N_1–N_2. At the end, the FCS measurements were mapped near an individual AuNP, and it was found that the near-field FCS effects can be observed in the range of ~±300 nm in the *xy* plane centered at the particle location. The range is comparable to that of the light diffraction limit. It should be noticed

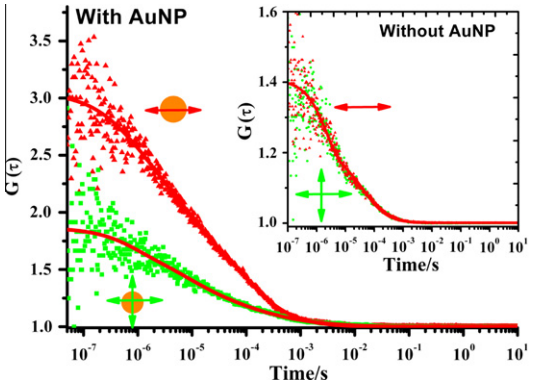

Figure 4. Typical original FCS autocorrelation data with a gold nanoparticle illuminated by the focused laser beam with linear polarization (red triangles) and circular polarization (green squares). The red lines are the fitting curves with Eq. (1). Inset figure shows the typical original FCS autocorrelation data without any AuNP and their fitting curves. (For interpretation of the references to colour in this figure legend, the reader is referred to the web version of this article.)

that the $G_{(0)}$ value and the diffusion time vary some for different individual AuNPs because of the differences between their size, shape, and bonding to the substrate surface. This topic will be discussed in detail in another work.

3.3. The near-field volume versus the polarization of the excitation light

Usually, the excitation of the nanostructure's surface plasmon resonance is dependent on the polarization of the excitation light. Here, the autocorrelation curves were measured with linear and circular polarizations of lights to investigate the variation of the near-field volume with different polarizations of light. The typical results are shown in Figure 4. Interestingly, the value of $G_{(0)}$ with the linear polarization light is obviously higher than that obtained with the circular polarization of light. This phenomenon implies that the near-field volume for the linear polarization of light is smaller than that for the circular polarization of light. Moreover, the diffusion time obtained by fitting the data with Eq. (1) for the linear polarization of light is shorter than that for the circular polarization of light. This confirms the conclusion of the near-field volume reducing which is indicated from the variation of the $G_{(0)}$ value. Obviously, the electromagnetic field distribution near the AuNP illuminated by a circular polarization of light should surround circularly the nanoparticle. The field distribution should be different from that generated by the light with linear polarization of light (Figure 1b). The variation of the near-field volume under different excitation polarized light points out a way to control the near-field volume in the vicinity of the AuNP experimentally. Furthermore, FCS measurements in the absence of AuNPs were also performed for comparison (see Figure 4 inset). The results on the bare glass surface are almost the same for the circular and the linear polarizations of lights, which is reasonable because of the fluorescence isotropic properties. This result is a proof that the FCS polarization dependence phenomenon near an AuNP is just only due to the surface plasmon resonance properties of the particle. The shapes of the most AuNPs used in this experiment, as shown in Figure 2a, are ellipses instead of perfectly spherical. This shape would result in polarization dependence phenomena for near-field FCS measurements (data not shown here). Except for the external light polarization, the shape of the nanostructure can also be tuned to control the near-field volume. This content is beyond the scope of the paper.

3.4. The FCS near single AuNP with various dye concentrations

Near-field FCS measurements in the vicinity of single AuNP were also performed for the fluorophore concentration varying from 4.5 nM to 150 μM. As can be seen from Figure 5a and b, the autocorrelation curves show similar behaviors as previously described. For instance, in the presence of an AuNP, there is an obvious increase of $G_{(0)}$ indicating a smaller the near-field volume and brighter fluorophore. The dye molecule diffusing through the enhancement region in the near field would result in additional fluorescence signal fluctuations, which leads to the changes of $G_{(0)}$ value and the shape of the autocorrelation curves. The molecular fluorescence intensity in the near-field volume still increases at the high dye concentration because the autocorrelation curves are modified definitely in presence of the AuNPs. Here, the fitting results of the FCS data show that there are also two different characteristic diffusion times, which means that the near-field enhancement still exists at various dye concentrations. Unexpectedly, the detected total fluorescent signal intensity is higher in the presence of the AuNPs than that in the absence of the AuNPs at the low dye concentrations, whereas the inverse situation appears at the high concentrations (Figure 5c). The transition concentration for this inverse is found as around 300 nM. To get insight

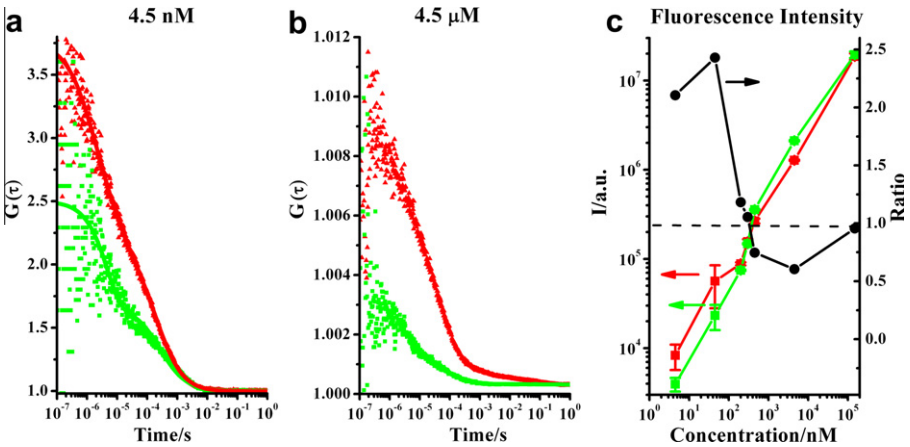

Figure 5. FCS autocorrelation curves in the present of AuNPs at different fluorophore concentrations. (a) and (b), typical original FCS autocorrelation data and the corresponding fitting curves with an AuNP (red triangles) and without any AuNP (green squares). (c) Fluorescence intensities at the various fluorophore concentrations. The red ones are for the experimental data with an AuNP, the green ones are for that without any AuNP, and the black ones indicate the ratio of the red ones to the corresponding green ones. (For interpretation of the references to colour in this figure legend, the reader is referred to the web version of this article.)

into this concentration dependence fluorescence, the fluorescence intensities are now reviewed as a function of the excitation laser powers at the low concentrations. The detected fluorescence intensity can be rewritten as $F_t \approx \int Q_c \cdot I_{1,r} \cdot (1 + \rho_r \cdot I_{2,r}/I_{1,r}) \cdot C_{r,t} dV$. At the low concentration (Figure 3b), the fluorescence intensity increases along with the excitation power in the presence of the AuNPs and possesses a higher slope than that without the AuNPs. This agrees well with the results detailed in Ref. [9] and can be explained as that the enhancement factor ρ_r dominates the variation of the fluorescence intensity at the low dye concentration. However, at the high dye molecule concentration, the absorbance of the excitation and the emission lights by the sample itself, $I = I_0 e^{-\varepsilon l C}$ (where ε is the molar absorption coefficient, l is the absorption path length, and C is the fluorophore concentration), has to be taken into account. The decrease of the total fluorescence intensity in the present of AuNPs should mainly due to the significant decreasing of the signal from the far-field volume. Because of the absorbance and the scattering of the AuNP, ε is larger in the presence of the AuNPs, so that the fluorescence intensity is expected to decrease at the high concentration.

4. Conclusion

In summary, we demonstrated the single molecule diffusion behaviors experimentally within the near-field volume of an individual gold nanoparticle illuminated by a tightly focused beam using FCS method. The near-field effect of an individual AuNP can be definitely observed with the method, and the diffusion kinetics of the fluorophore within the near-field volume was analyzed theoretically by a simple approximation model. Such a reduced near-field volume of the AuNP is of benefit to the local dynamics study with a high spatial resolution, and the signal noise ratio of FCS convolved with AuNPs can be increased by enhancing the photons counts per molecule [9]. The contrast between the near-field signal around the particle and the far-field signal excited directly by the objective lens could be enhanced by two-photon fluorescence process, because the fluorescence signal is proportional to the square of the exciting laser intensity [30]. Furthermore, the AuNPs are more compatible material for biology so that it is suitable to enter into an organism of interest by diffusion process or under the manipulation of an optical trapping force or a scanning fiber probe attached with one particle [31–33]. In principle, the experimental scheme with single AuNP could be applied in cell biology to analyze membrane, even the intracellular processes in a living cell.

Acknowledgement

This research was supported by National Natural Science Foundation of China (10821062, 90921008, 61008026), National Basic Research Program of China (2007CB307001) and China Postdoctoral Science Foundation (20100470140).

References

[1] D. Magde, E. Elson, W.W. Webb, Phys. Rev. Lett. 29 (1972) 705.
[2] R. Rigler, U. Mets, J. Widengren, P. Kask, Eur. Biophys. J. Biophys. Lett. 22 (1993) 169.
[3] Sudipta Maiti, Ulrich Haupts, Watt W. Webb, Proc. Natl. Acad. Sci. USA 94 (1997) 11753.
[4] K. Bacia, S.A. Kim, P. Schwille, Nat. Methods 3 (2006) 83.
[5] L. Kastrup, H. Blom, C. Eggeling, S.W. Hell, Phys. Rev. Lett. 94 (2005) 178104.
[6] M. Foquet, J. Korlach, W.R. Zipfel, W.W. Webb, H.G. Craighead, Anal. Chem. 76 (2004) 1618.
[7] N.L. Thompson, B.L. Steele, Nat. Protoc. 2 (2007) 878.
[8] M.J. Levene, J. Korlach, S.W. Turner, M. Foquet, H.G. Craighead, W.W. Webb, Science 299 (2003) 682.
[9] H. Rigneault et al., Phys. Rev. Lett. 95 (2005) 117401.
[10] M. Leutenegger, M. Gosch, A. Perentes, P. Hoffmann, O.J.F. Martin, T. Lasser, Opt. Express 14 (2006) 956.
[11] A. Lewis, Y.Y. Kuttner, R. Dekhter, M. Polhan, Isr. J. Chem. 47 (2007) 171.
[12] D. Vobornik, D.S. Banks, Z. Lu, C. Fradin, R. Taylor, L.J. Johnston, Appl. Phys. Lett. 93 (2008) 163904.
[13] G.W. Lu, F.H. Lei, J.F. Angiboust, M. Manfait, Eur. Biophys. J. 39 (2010) 855.
[14] M. Herrmann, N. Neuberth, J. Wissler, J. Ṕerez, D. Gradl, A. Naber, Nano Lett. 9 (2009) 3330.
[15] H. Rigneault, P. Lenne, J. Opt. Soc. Am. B 20 (2003) 2203.
[16] D. Julie, G. Samuel, L.F. Sandrine, S. Neso, F. Emmanuel, Proc. SPIE 7571 (2010) 757114.
[17] F.D. Stefani, K. Vasilev, N. Bocchio, N. Stoyanova, M. Kreiter, Phys. Rev. Lett. 94 (2005) 023005.
[18] J. Zhang, Y. Fu, M.H. Chowdhury, J.R. Lakowicz, Nano Lett. 7 (2007) 2101.
[19] O.L. Muskens, V. Giannini, J.A. Sánchez-Gil, J. Gómez Rivas, Nano Lett. 7 (2007) 2871.
[20] L.C. Estrada, P.F. Aramendía, O.E. Martínez, Opt. Express 16 (2008) 20597.
[21] A. Kinkhabwala, Z. Yu, S. Fan, Y. Avlasevich, K. Mullen, W.E. Moerner, Nat. Photonics 3 (2009) 654.
[22] V. Jacobsen, P. Stoller, C. Brunner, V. Vogel, V. Sandoghdar, Opt. Express 14 (2006) 405.
[23] P. Anger, P. Bharadwaj, L. Novotny, Phys. Rev. Lett. 96 (2006) 113002.
[24] T. Hartling, P. Reichenbach, L.M. Eng, Opt. Express 15 (2007) 12806.
[25] O. Krichevsky, G. Bonnet, Rep. Prog. Phys. 65 (2002) 251.
[26] C. Fradin, A. Abu-Arish, R. Granek, M. Elbaum, Biophys. J. 84 (2003) 2005.
[27] G. Frens, Nat. Phys. Sci. 241 (1973) 20.
[28] K.C. Grabar et al., J. Am. Chem. Soc. 118 (1996) 1148.
[29] J. Widengren, P. Schwille, J. Phys. Chem. A. 104 (2000) 6416.
[30] K.M. Berland, P.T.C. So, E. Gratton, Biophys. J. 68 (1995) 694.
[31] T. Kalkbrenner, M. Ramstein, J. Mlynek, V. Sandoghdar, J. Microsc. 202 (2001) 72.
[32] K. Svoboda, S.M. Block, Opt. Lett. 19 (1994) 930.
[33] T. Sugiura, T. Okada, Y. Inouye, O. Nakamura, S. Kawata, Opt. Lett. 22 (1997) 1663.